The Astrophysical Journal Letters, 790:L28 (5pp), 2014 August 1 doi:10.1088/2041-8205/790/2/L28

DETECTION OF 36 GHz CLASS I METHANOL MASER EMISSION TOWARD NGC 253

Simon P. Ellingsen[1], Xi Chen[2,3], Hai-Hua Qiao[2,4], Willem Baan[2], Tao An[2,3], Juan Li[2,3], and Shari L. Breen[5]
[1] School of Physical Sciences, University of Tasmania, Hobart, Tasmania, Australia; Simon.Ellingsen@utas.edu.au
[2] Shanghai Astronomical Observatory, Chinese Academy of Sciences, Shanghai 200030, China
[3] Key Laboratory of Radio Astronomy, Chinese Academy of Sciences, Nanjing, JiangSu 210008, China
[4] University of Chinese Academy of Sciences, 19A Yuquanlu, Beijing 100049, China
[5] CSIRO Astronomy and Space Science, Australia Telescope National Facility, P.O. Box 76, Epping, NSW 1710, Australia
Received 2014 June 11; accepted 2014 July 7; published 2014 July 17

ABSTRACT

We have used the Australia Telescope Compact Array to search for emission from the $4_{-1} \rightarrow 3_0E$ transition of methanol (36.2 GHz) toward the center of the nearby starburst galaxy NGC 253. Two regions of emission were detected, offset from the nucleus along the same position angle as the inner spiral arms. The emission is largely unresolved on a scale of 5″, has a FWHM line width of <30 km s^{-1}, and an isotropic luminosity orders of a magnitude larger than that observed in any Galactic star formation region. These characteristics suggest that the 36.2 GHz methanol emission is most likely a maser, although observations with higher angular and spectral resolution are required to confirm this. If it is a maser, this represents the first detection of a class I methanol maser outside the Milky Way. The 36.2 GHz methanol emission in NGC 253 has more than an order of magnitude higher isotropic luminosity than the widespread emission recently detected toward the center of the Milky Way. If emission from this transition scales with the nuclear star formation rate, then it may be detectable in the central regions of many starburst galaxies. Detection of methanol emission in ultra-luminous infrared galaxies would open up a new tool for testing for variations in fundamental constants (particularly the proton-to-electron mass ratio) on cosmological scales.

Key words: galaxies: individual (NGC 253) – galaxies: starburst – masers – radio lines: ISM

Online-only material: color figure

1. INTRODUCTION

Methanol is a commonly observed species in interstellar gas, and its rich microwave and millimeter spectrum has made it a powerful tool for studying high-mass star formation through its numerous masing transitions (e.g., Ellingsen et al. 2012a), while thermal methanol emission is often observed toward hot molecular cores (e.g., van der Tak et al. 2000).

It has recently been discovered that observations of rotational transitions of methanol provide particularly sensitive tests for variations in the proton-to-electron mass ratio (μ) (Jansen et al. 2011; Levshakov et al. 2011). Although readily observable in the local universe, the only detections of methanol emission beyond the Milky Way are a small number of masers from the 6.7 GHz transition toward the Large Magellanic Cloud (LMC; Green et al. 2008) and M31 (Sjouwerman et al. 2010), one 12.2 GHz maser in the LMC (Ellingsen et al. 2010), absorption in the 6.7 GHz transition toward the center of NGC 3079 (Impellizzeri et al. 2008), and thermal emission toward the nearby galaxies NGC 253, IC342, Maffei 2, NGC 6946, NGC 4945, and M82 (Henkel et al. 1987, 1990; Hüttemeister et al. 1997; Martín et al. 2006). Methanol absorption has been detected in a number of transitions toward the lensing galaxy ($z = 0.89$) in the PKS B 1830-211 gravitational lens system (Ellingsen et al. 2012b; Bagdonaite et al. 2013; Muller et al. 2014) and these observations have been used to place tight constraints on variations in μ in this system (Bagdonaite et al. 2013). However, strong lensing systems such as PKS B1830-211 are rare, so an alternative approach for detecting methanol at high redshifts is desirable.

Some active galaxies show strong maser emission from either the 1667 MHz OH or the 22 GHz water transitions. These masers are in some cases more than a million times more luminous than typical galactic masers observed in star formation regions or late-type stars and for this reason are referred to as megamasers. OH megamasers are observed toward the nuclear regions of ultra-luminous infrared galaxies (ULIRGS), systems undergoing merger activity (e.g., Baan et al. 1982), while water masers are observed in accretion disks and jets toward low-luminosity active galactic nuclei (AGNs), typically Seyfert 2 galaxies (e.g., Miyoshi et al. 1995). A number of unsuccessful searches for methanol megamasers have been undertaken (Ellingsen et al. 1994; Phillips et al. 1998; Darling et al. 2003); these have all focused on the 6.7 GHz ($5_1 \rightarrow 6_0A^+$) transition of methanol, the strongest and most common transition in galactic star-formation regions. The targets for these searches were primarily known OH and water megamaser systems.

Methanol maser transitions are empirically divided into two classes based on their environments and pumping mechanisms. Class I masers are collisionally pumped where outflows or other low-energy shocks interact with dense molecular gas. In general, multiple discrete maser sites are observed toward a single star-formation region, distributed on scales of around 1 pc (Kurtz et al. 2004; Voronkov et al. 2014). Class II masers are radiatively pumped and are closely associated with infrared sources, OH, and water masers. Generally, only one or two sites are observed in a given star-formation region and the masers are distributed on scales an order of magnitude smaller than the class I masers. The class II methanol masers are exclusively associated with high-mass star-formation regions (Breen et al. 2013), whereas class I masers have also been observed associated with lower-mass young stars (Kalenskii et al. 2010) and recently have also been detected associated with supernova remnants (Pihlström et al. 2014). To date, there have been no reported searches for extragalactic class I masers.

Recently, Yusef-Zadeh et al. (2013) detected widespread emission from the $4_{-1} \rightarrow 3_0E$ class I maser transition of methanol (which we hereafter call the 36.2 GHz methanol

transition) in the inner region of the Milky Way. Observations with the Very Large Array detected more than 350 separated sites in a 160 × 43 pc region, with an integrated luminosity over the whole region in excess of 5600 Jy km s^{-1}. The 36.2 GHz class I methanol maser transition was first detected toward galactic star-formation regions (Haschick & Baan 1989) and is one of the most common and strongest class I methanol masers (Voronkov et al. 2014). Yusef-Zadeh et al. (2013) suggest that the large number of 36.2 GHz methanol masers in the central molecular zone (CMZ) of the Milky Way is due to enhanced methanol abundance in this region produced by photodesorption of methanol from cold dust by cosmic rays. It is likely that similar mechanisms operate in other galaxies, and furthermore that galaxies with enhanced star formation in their central regions may exhibit 36.2 GHz emission over larger volumes that may be readily detectable. Interestingly, more than 20 yr ago, Sobolev (1993) suggested that the 36.2 GHz class I methanol transition provided the best prospect for producing methanol megamasers.

In this Letter, we report a search for 36.2 GHz methanol emission from the central region of NGC 253, a nearby spiral galaxy that has significant starburst activity toward its center (see Sakamoto et al. 2011, and references therein). NGC 253 has been studied in detail at a wide range of wavelengths, including radio (e.g., Ulvestad & Antonucci 1997), millimeter (e.g., Bolatto et al. 2013), infrared (e.g., Dale et al. 2009), optical (e.g., Dalcanton et al. 2009), and x-ray (e.g., Strickland et al. 2000). Large amounts of molecular gas have been detected toward the central region of the galaxy (Mauersberger et al. 1996), with more than 25 different molecular species having been observed (e.g., Martín et al. 2006), including the first detection of methanol emission beyond the Milky Way (Henkel et al. 1987). We have adopted a distance estimate of 3.4 Mpc for NGC 253 in this work (Dalcanton et al. 2009).

2. OBSERVATIONS

The observations were made using the Australia Telescope Compact Array (ATCA) on 2014 March 29 (project code C2879). The array was in the H168 configuration (baseline lengths between 61 and 192 m) and the synthesized beam width for the observations at 36 GHz was approximately 8.″0 × 4.″2. The Compact Array Broadband Backend (Wilson et al. 2011) was configured with 2 × 2.048 GHz bands centered on frequencies of 35.3 and 37.3 GHz, respectively. Each of the bands was divided into 2048 spectral channels each of 1 MHz bandwidth, corresponding to a spectral resolution of 9.9 km s^{-1} at 36.2 GHz for uniform weighting of the correlation function (a channel width of 8.2 km s^{-1}). The 2.048 GHz bands cover the rest frequencies of the $4_{-1} \rightarrow 3_0E$ and $7_{-2} \rightarrow 8_{-1}E$ transitions of methanol, for which we adopted rest frequencies of 36.169265 and 37.703700 GHz, respectively (Müller et al. 2004).

The data were reduced with MIRIAD using the standard techniques for ATCA observations. Amplitude calibration was with respect to Uranus and PKS B1921-293 was observed as the bandpass calibrator. The data were corrected for atmospheric opacity and the absolute flux density calibration is estimated to be accurate to 30%. The observing strategy interleaved 10 minutes on NGC 253 (pointing center $\alpha = 00^{\rm h}47^{\rm m}33^{\rm s}.10$; $\delta = -25^\circ17'18''.0$ (J2000)) with 2 minute observations of a nearby phase calibrator (0116-219) before and after the target source. The total duration of the on-source time for NGC 253 was 30 minutes. The data from the two bands were combined during imaging to yield a total bandwidth of ∼3.9 GHz. Continuum emission from the center of NGC 253 was then used to produce a model for self-calibration. After self-calibration, continuum subtraction was undertaken prior to imaging the 36.2 and 37.7 GHz methanol maser transitions at full spectral resolution. The resulting rms noise in a single 1 MHz (8.2 km s^{-1}) spectral channel for the 36.2 GHz methanol transition was $\lesssim$0.8 mJy beam^{-1}.

Additional observations were undertaken in a director's time allocation on 2014 May 18. The array was in the 1.5D configuration (baseline lengths between 107 and 1469 m). We obtained a further 30 minutes on-source on NGC 253, but with very limited hour-angle coverage (approximately 45 minutes). The amplitude and bandpass calibration were performed in the same manner as for the March observations.

3. RESULTS

The continuum emission from the central region of NGC 253 was detected as a point source in our observations with an integrated intensity of 0.11 Jy. Molecular emission within the CMZ of NGC 253 spans a velocity range from ∼100 to 400 km s^{-1} (Sakamoto et al. 2011) and we imaged a velocity range covering barycentric velocities in the range of −150 to 670 km s^{-1} for the 36.2 GHz methanol transition at 8.2 km s^{-1} velocity resolution. Figure 1 (right) shows the both the 36 GHz continuum emission (green contours) and the integrated 36.2 GHz methanol emission (red contours) with a *Spitzer* Infrared Array Camera (IRAC) three-color image as the background (Dale et al. 2009). The 36.2 GHz methanol emission was detected in both observing epochs; however, for the May 18 observations, the purely east–west baseline configuration and limited hour angle range mean that it cannot be used for imaging and the data presented here are only from the March 29 observations. For the May 18 observations, the 36.2 GHz emission is observed on all baselines shorter than 25 kλ, but not on the longer baselines. As the line emission is detected with relatively low signal to noise in a 30 minute observation, it is not possible to determine from our data if the non-detection on longer baselines is because the emission is resolved or if it is due to atmospheric decorrelation.

The continuum emission is clearly associated with the nucleus of NGC 253, while the methanol emission is offset. At the resolution of our observations, we detect two regions of 36.2 GHz methanol emission (Table 1), significantly offset from the nucleus, but lying along the same position angle as the inner spiral arms traced by the mid-infrared emission.

The observations of the 37.7 GHz methanol transition found no emission with a 5σ limit of approximately 3 mJy beam^{-1} in a single 1 MHz spectral channel. The 37.7 GHz transition of methanol is observed as a relatively rare and weak class II maser in Galactic star-formation regions (e.g., Ellingsen et al. 2011b), so its non-detection here is expected. This transition was only included because it could be observed simultaneously with the 36.2 GHz transition and we do not discuss it further here.

The methanol emission offset from the nucleus toward the northeast (hereafter Meth NE) is associated with two ammonia cores (Lebrón et al. 2011) and is close to one of two water masers detected toward NGC 253 by Henkel et al. (2004), the locations of which are marked in Figure 1 with blue crosses. Meth NE is offset from the center of NGC 253 by 11.″1, which for an assumed distance of 3.4 Mpc corresponds to 180 pc. The other methanol emission toward the southwest (hereafter Meth SW) is offset from the center by 18.″4 (300 pc), is associated

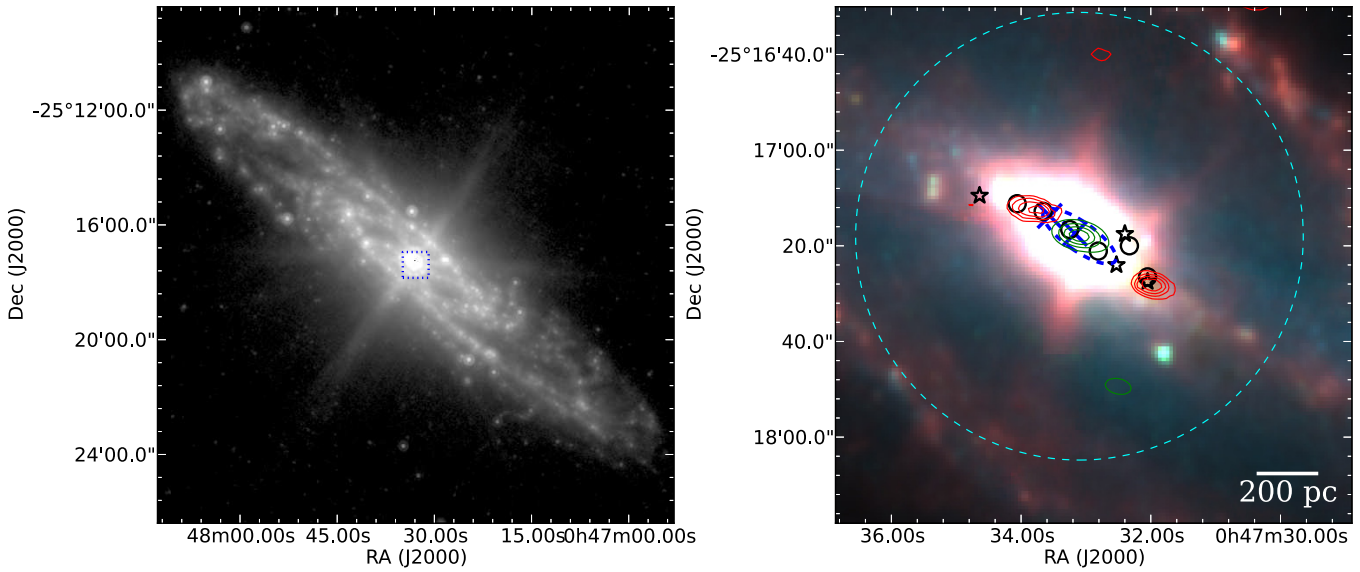

Figure 1. Left: *Spitzer* 24 μm image of NGC 253 (Dale et al. 2009). The blue box marks the region shown in the right-hand panel. Right: 36 GHz continuum emission (green contours at 20%, 40%, 60%, and 80% of 95 mJy beam^{-1}) and 36.2 GHz methanol emission (red contours 20%, 40%, 60%, and 80% of 310 mJy km s^{-1} beam^{-1}). The dashed blue ellipse marks the half-maximum intensity of the central molecular zone of NGC 253 (Sakamoto et al. 2011). The background image is from *Spitzer* IRAC observations with blue, green, and red from the 3.6, 4.5, and 8.0 μm bands, respectively (Dale et al. 2009). The blue crosses mark the location of water masers detected by Henkel et al. (2004), the black stars mark supershells identified by Sakamoto et al. (2006) and Bolatto et al. (2013), and the black circles mark NH_3 cores (Lebrón et al. 2011). The cyan dashed line shows the size of the primary beam of the ATCA observations.

(A color version of this figure is available in the online journal.)

Table 1
36.2 GHz Emission toward NGC 253

Name	Right Ascension (^{h} ^{m} ^{s})	Declination ($^\circ$ $'$ $''$)	Peak Flux (mJy)	Integrated Flux (mJy km s^{-1})	Peak Velocity (km s^{-1})	Velocity Range (km s^{-1})
Meth. NE	00:47:33.8	−25:17:12	10.5	310 ± 50	194	88 – 211
Meth. SW	00:47:32.0	−25:17:28	8.7	310 ± 50	350	285 – 350
Continuum	00:47:33.1	−25:17:18	93	110		

with an ammonia core, and is close to the site of a supershell identified by Bolatto et al. (2013).

4. DISCUSSION

4.1. The Nature of the 36 GHz Methanol Emission

These observations represent the first detection of methanol emission from the $4_{-1} \rightarrow 3_0E$ from a source beyond the Milky Way. A key question to address is whether the 36.2 GHz methanol emission sites in NGC 253 are produced by maser or thermal processes. Figure 2 compares the spectra of the 36.2 GHz methanol emission to those from CO(2–1) toward the same location (Sakamoto et al. 2011). It is clear from Figure 2 that the velocity of the methanol emission is close to peak of the CO(2–1) from the same direction, but covers a significantly smaller velocity range. Previous observations with similar angular resolution have detected methanol emission toward the central regions of NGC 253 with FWHM line widths of around 100 km s^{-1} (Henkel et al. 1987; Martín et al. 2006). In contrast, for the 36.2 GHz methanol emission in Figure 2, the lines are narrow, with widths of the order of the spectral resolution of our observations (∼10 km s^{-1}).

The isotropic luminosity of Milky Way class I methanol masers associated with star-formation regions is typically less than 500 Jy km s^{-1} kpc^2, while the integrated 36.2 GHz methanol emission from the Milky Way CMZ is three orders of magnitude greater. We measure an integrated intensity of 0.62 Jy km s^{-1} for the 36.2 GHz methanol emission toward the central region of NGC 253 (Table 1), which for a distance of 3.4 Mpc corresponds to an isotropic luminosity of 7.2×10^6 Jy km s^{-1} kpc^2. At a distance of 8.5 kpc, this would correspond to an integrated intensity of approximately 10^5 Jy km s^{-1}. Hence the 36.2 GHz methanol emission toward the center of NGC 253 is a factor of more than 17 greater than the emission in the Milky Way CMZ, much, perhaps most, of which is known to be due to maser sources.

Figure 1 shows that the two methanol emission regions are compact and essentially unresolved at the resolution of these observations. Using the Rayleigh-Jeans approximation, the factor to convert an unresolved source of this angular size from a flux density to the temperature scale is 40 K Jy^{-1}. Martín et al. (2006) detected multiple thermal transitions of methanol in the 2 mm band toward the center of NGC 253. Assuming optically thin emission for the observed methanol transitions, Martín et al. used rotation diagram analysis to derive a column density and rotation temperature of 8.3×10^{14} cm^{-2} and 11.6 K, respectively. Using these values, we can estimate the integrated intensity to expect in the 36.2 GHz transition if the emission is thermal. We calculate an integrated intensity of 0.8 K km s^{-1} for thermal emission from the 36.2 GHz transition; however, we observe an integrated intensity of 25 K km s^{-1} (corresponding to 0.62 Jy km s^{-1}; see Table 1). So the integrated emission we observe from the 36.2 GHz methanol transition is about 30 times greater than

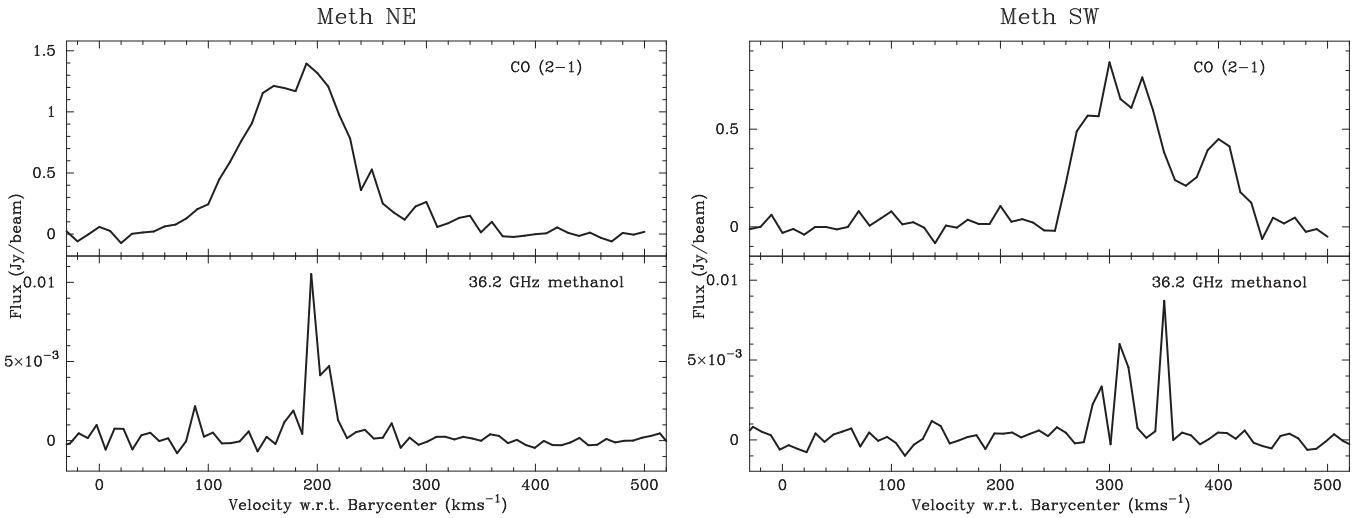

Figure 2. Comparison of the 36.2 GHz methanol emission from the current observations with the CO(2–1) emission from the same region Sakamoto et al. (2011).

predicted if it were due to thermal emission similar to that previously observed from methanol in NGC 253.

The combination of high isotropic luminosity (well in excess of the expectations for thermal emission), and the narrow line width of the 36.2 GHz methanol emission in NGC 253 is highly suggestive that it is maser emission. However, additional observations with higher spectral and angular resolution are required to verify that the 36.2 GHz methanol emission in NGC 253 is a maser.

4.2. Comparison with the Milky Way CMZ Methanol Emission

The CMZ in NGC 253 is observed to have an extent (to half-maximum intensity) of about 300 × 100 pc (indicated by a blue dashed ellipse in Figure 1; Sakamoto et al. 2011) and the two regions of 36.2 GHz methanol emission identified here lie beyond that. This is within the region where H_2CO absorption is observed (Baan et al. 1997) and close the outer extent of emission from dense gas tracers such as HCN, HCO^+, and NH_3 (Knudsen et al. 2007; Lebrón et al. 2011). The mechanism proposed by Yusef-Zadeh et al. (2013) to explain Milky Way CMZ 36.2 GHz methanol masers requires the presence of cold dust (to form or host methanol-rich ices) and an enhanced cosmic ray flux (compared to the galactic disk). Yusef-Zadeh et al. (2013) found that high cosmic ray intensities desorb methanol from cold dust grains, but if the intensity is too high they are rapidly destroyed once they are released into the gas phase. They explain the low density of 36.2 GHz methanol emission within the circumnuclear ring of the Milky Way as perhaps being due to this. The absence of any strong 36.2 GHz methanol emission in the inner 100 pc in NGC 253 may be because within that region, gas-phase methanol is rapidly destroyed. This would imply that the flux of cosmic rays and/or energetic photons are at extreme levels over a much larger volume than in the Milky Way, which is plausible given the high supernova rate estimated for this region (Lenc & Tingay 2006). Alternatively, there is evidence that the edges of the inner molecular disk in NGC 253 are affected by the nuclear outflow and the 36.2 GHz methanol emission may be being produced by that interaction. Methanol is released from dust grains in slow shocks and this has previously been suggested as the mechanism responsible for the presence of easily dissociated molecules in the central region of NGC 253 (Lebrón et al. 2011) and the close association of both sites of 36.2 GHz methanol emission with NH_3 cores supports this hypothesis (Figure 1). A third possibility is that the 36.2 GHz methanol emission sites correspond to regions where there is a large number of very young high-mass star-formation regions within a small volume and the Meth SW emission is close to a supershell (Bolatto et al. 2013). However, in terms of the intensity of the dust continuum and mid-infrared emission, the two methanol emission sites are much weaker than regions closer to the NGC 253 nucleus, which is inconsistent with them being locations of unusual star formation activity within the central regions of NGC 253. So the observed methanol emission sites likely represent regions where there is an appropriate balance between the cold dust where methanol is produced through grain surface reactions and the presence of cosmic rays or slow shocks to release it into the gas phase.

4.3. Prospects for 36.2 GHz Methanol Megamasers

The star formation rate in NGC 253 has been estimated from the infrared luminosity to be 3.6 $M_\odot$ yr^{-1} (Strickland et al. 2004), significantly higher than recent estimates of 0.68–1.45 $M_\odot$ yr^{-1} for the Milky Way determined from *Spitzer* observations (Robitaille & Whitney 2010). However, the starburst activity in NGC 253 is relatively modest and more distant, interacting galaxies exhibit star formation rates up to two or three orders of magnitude greater. The detected 36.2 GHz methanol emission toward the center of NGC 253 has an isotropic luminosity four orders of magnitude stronger than that observed from typical class I masers in galactic star-formation regions, so it does not classify as a methanol megamaser. However, it is more than an order of magnitude stronger than the integrated 36.2 GHz methanol emission from the Milky Way CMZ, which suggests that emission from this transition may scale with the star formation rate. Additional observations of other nearby starburst systems are clearly required to determine if this is the case and to assess the specific factors that govern the luminosity of the 36.2 GHz methanol emission. The detection of 36.2 GHz methanol masers in the Milky Way CMZ and NGC 253 suggests that galaxies with large amounts of cold dust and high star formation rates within their central regions (e.g., ULIRGs) may host large volumes conducive to enhanced 36.2 GHz methanol emission.

As outlined in the Introduction, one motivation for searching for methanol emission at cosmological distances is that it is unusually sensitive to variations in the proton-to-electron mass ratio μ. The sensitivity coefficient K_μ for the 36.2 GHz $4_{-1} \rightarrow 3_0 E$ transition is approximately 10 (Jansen et al. 2011; Levshakov et al. 2011), an order of magnitude larger than a pure rotational transition. Different methanol transitions have different sensitivities to variations in μ and, as discussed by Ellingsen et al. (2011a), comparison between methanol maser transitions is able to provide constraints with far fewer sources of systematic uncertainty than comparisons between different molecular species. The 84.5 GHz $5_{-1} \rightarrow 4_0 E$ transition ($K_\mu \sim 3.5$; Levshakov et al. 2011) and the 229 GHz $8_{-1} \rightarrow 7_0 E$ transition are in the same family as the 36.2 GHz transition and are observed as class I masers in galactic star-formation regions. If the 36.2 GHz $4_{-1} \rightarrow 3_0 E$ transition is detected as a megamaser at cosmological distances, then sensitive searches for the 84.5 and 229 GHz transitions should be undertaken to determine whether they can also be observed in these systems.

5. CONCLUSIONS

We have made the first search for the 36.2 GHz $4_{-1} \rightarrow 3_0 E$ methanol transition toward the nearby starburst Galaxy NGC 253. We detect two regions of emission close to, but offset from, the nuclear region. The line width and luminosity compared to previous observations of thermal methanol emission in NGC 253 suggest that the 36.2 GHz emission regions are likely masers, although further data are required to confirm this. If the 36.2 GHz emission is from masers, then this represents the first detection of class I methanol masers outside the Milky Way and the first detection of any methanol maser at distances greater than 1 Mpc. If emission from this transition scales with the star formation rate, then it may be possible to detect it at cosmological distances and use it to test for variations in the fundamental constants.

Xi Chen acknowledges support from the National Natural Science Foundation of China (11133008 and 11273043), the Strategic Priority Research Program of the Chinese Academy of Sciences (CAS; grant No. XDA04060701), Key Laboratory for Radio Astronomy, CAS. Shari Breen is the recipient of an Australian Research Council DECRA Fellowship (project No. DE130101270). The Australia Telescope Compact Array is part of the Australia Telescope National Facility, which is funded by the Commonwealth of Australia for operation as a National Facility managed by CSIRO.

REFERENCES

Baan, W. A., Bragg, A. E., Henkel, C., & Wilson, T. L. 1997, ApJ, 491, 134
Baan, W. A., Wood, P. A. D., & Haschick, A. D. 1982, ApJL, 260, L49
Bagdonaite, J., Jansen, P., Henkel, C., et al. 2013, Sci, 339, 46
Bolatto, A. D., Warren, S. R., Leroy, A. K., et al. 2013, Natur, 499, 450
Breen, S. L., Ellingsen, S. P., Contreras, Y., et al. 2013, MNRAS, 435, 524
Dalcanton, J. J., Williams, B. F., Seth, A. C., et al. 2009, ApJS, 183, 67
Dale, D. A., Cohen, S. A., Johnson, L. C., et al. 2009, ApJ, 703, 517
Darling, J., Goldsmith, P., Li, D., & Giovanelli, R. 2003, AJ, 125, 1177
Ellingsen, S., Voronkov, M., & Breen, S. 2011a, PhRvL, 107, A270801
Ellingsen, S. P., Breen, S. L., Caswell, J. L., Quinn, L. J., & Fuller, G. A. 2010, MNRAS, 404, 779
Ellingsen, S. P., Breen, S. L., Sobolev, A. M., et al. 2011b, ApJ, 742, 109
Ellingsen, S. P., Norris, R. P., Whiteoak, J. B., et al. 1994, MNRAS, 267, 510
Ellingsen, S. P., Sobolev, A. M., Cragg, D. M., & Godfrey, P. D. 2012a, ApJ, 759, L5
Ellingsen, S. P., Voronkov, M. A., Breen, S. L., & Lovell, J. E. J. 2012b, ApJL, 747, L7
Green, J. A., Caswell, J. L., Fuller, G. A., et al. 2008, MNRAS, 385, 948
Haschick, A. D., & Baan, W. A. 1989, ApJ, 339, 949
Henkel, C., Jacq, T., Mauersberger, R., Menten, K. M., & Steppe, H. 1987, A&A, 188, L1
Henkel, C., Tarchi, A., Menten, K. M., & Peck, A. B. 2004, A&A, 414, 117
Henkel, C., Whiteoak, J. B., Nyman, L.-A., & Harju, J. 1990, A&A, 230, L5
Hüttemeister, S., Mauersberger, R., & Henkel, C. 1997, A&A, 326, 59
Impellizzeri, C. M. V., Henkel, C., Roy, A. L., & Menten, K. M. 2008, A&A, 484, L43
Jansen, P., Xu, L.-H., Kleiner, I., Ubachs, W., & Bethlem, H. L. 2011, PhRvL, 106, 100801
Kalenskii, S. V., Johansson, L. E. B., Bergman, P., et al. 2010, MNRAS, 405, 613
Knudsen, K. K., Walter, F., Weiss, A., et al. 2007, ApJ, 666, 156
Kurtz, S., Hofner, P., & Álvarez, C. V. 2004, ApJS, 155, 149
Lebrón, M., Mangum, J. G., Mauersberger, R., et al. 2011, A&A, 534, A56
Lenc, E., & Tingay, S. J. 2006, AJ, 132, 1333
Levshakov, S. A., Kozlov, M. G., & Reimers, D. 2011, ApJ, 738, 26
Martín, S., Mauersberger, R., Martín-Pintado, J., Henkel, C., & García-Burillo, S. 2006, ApJS, 164, 450
Mauersberger, R., Henkel, C., Wielebinski, R., Wiklind, T., & Reuter, H.-P. 1996, A&A, 305, 421
Miyoshi, M., Moran, J., Herrnstein, J., et al. 1995, Natur, 373, 127
Müller, H. S. P., Menten, K. M., & Mäder, H. 2004, A&A, 428, 1019
Muller, S., Combes, F., Guelin, M., et al. 2014, A&A, 566, A112
Phillips, C. J., Norris, R. P., Ellingsen, S. P., & Rayner, D. P. 1998, MNRAS, 294, 265
Pihlström, Y. M., Sjouwerman, L. O., Frail, D. A., et al. 2014, AJ, 147, 73
Robitaille, T. P., & Whitney, B. A. 2010, ApJL, 710, L11
Sakamoto, K., Ho, P. T. P., Iono, D., et al. 2006, ApJ, 636, 685
Sakamoto, K., Mao, R.-Q., Matsushita, S., et al. 2011, ApJ, 735, 19
Sjouwerman, L. O., Murray, C. E., Pihlström, Y. M., Fish, V. L., & Araya, E. D. 2010, ApJL, 724, L158
Sobolev, A. M. 1993, AstL, 19, 293
Strickland, D. K., Heckman, T. M., Colbert, E. J. M., Hoopes, C. G., & Weaver, K. A. 2004, ApJ, 606, 829
Strickland, D. K., Heckman, T. M., Weaver, K. A., & Dahlem, M. 2000, AJ, 120, 2965
Ulvestad, J. S., & Antonucci, R. R. J. 1997, ApJ, 488, 621
van der Tak, F. F. S., van Dishoeck, E. F., Evans, N. J., II, & Blake, G. A. 2000, ApJ, 537, 283
Voronkov, M. A., Caswell, J. L., Ellingsen, S. P., Green, J. A., & Breen, S. L. 2014, MNRAS, 439, 2584
Wilson, W. E., Ferris, R. H., Axtens, P., et al. 2011, MNRAS, 416, 832
Yusef-Zadeh, F., Cotton, W., Viti, S., Wardle, M., & Royster, M. 2013, ApJL, 764, L19